Development of hyaluronan-based dissolving microneedle arrays for dermal vaccination

Leone, M.

Chapter 6

Diphtheria toxoid dissolving microneedle vaccination: adjuvant screening and effect of repeated-fractional dose administration

Adapted from Int J Pharm 2020 (580): 119182

Mara Leone[1], Stefan Romeijn[1], Guangsheng Du[1], Sylvia E. Le Dévédec[2], Hilde Vrieling[1,4], Conor O'Mahony[3], Joke A. Bouwstra[1,*], Gideon Kersten[1,4,*]

[1] Division of BioTherapeutics, Leiden Academic Centre for Drug Research, Leiden University, the Netherlandsb

[2] Division of Drug Discovery and Safety, Leiden Academic Centre for Drug Research, Leiden University, the Netherlands

[3] Tyndall National Institute, University College Cork, Cork, Ireland

[4] Institute for Translational Vaccinology, Bilthoven, the Netherlands

[*] These authors contributed equally.

ABSTRACT

In this study the effect of repeated-fractional intradermal administration of diphtheria toxoid (DT) compared to a single administration in the presence or absence of adjuvants formulated in dissolving microneedles (dMNs) was investigated. Based on an adjuvant screening with a hollow microneedle (hMN) system, poly(I:C) and gibbsite, a nanoparticulate aluminum salt, were selected for further studies: they were co-encapsulated with DT in dMNs with either a full or fractional DT-adjuvant dose. Sharp dMNs were prepared regardless the composition and were capable to penetrate the skin, dissolve within 20 min and deposit the intended antigen-adjuvant dose, which remained in the skin for at least 5 h. Dermal immunization with hMN in repeated-fractional dosing (RFrD) resulted in a higher immune response than a single-full dose (SFD) administration. Vaccination by dMNs led overall to higher responses than hMN but did not show an enhanced response after RFrD compared to a SFD administration. Co-encapsulation of the adjuvant in dMNs did not increase the immune response further. Immunization by dMNs without adjuvant gave a comparable response to subcutaneously injected DT-$AlPO_4$ in a 15 times higher dose of DT, as well as subcutaneous injected DT-poly(I:C) in a similar DT dose. Summarizing, adjuvant-free dMNs showed to be a promising delivery tool for vaccination performed in SFD administration.

GRAPHICAL ABSTRACT

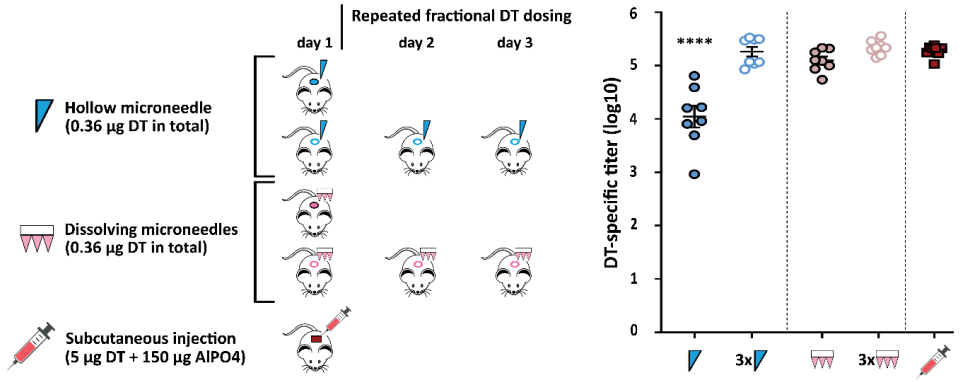

Keywords: dissolving microneedles, diphtheria toxoid, intradermal immunization, microneedles, aluminum-based adjuvants, repeated-fractional vaccine delivery.

1. INTRODUCTION

Vaccination has led to the control of devastating diseases such as smallpox, poliomyelitis, measles and hepatitis [1-3]. Most vaccines are injected intramuscularly or subcutaneously. However, classical injection can cause pain, distress, needle-stick injuries and requires trained personnel [4]. To overcome problems related to the hypodermic needles, less invasive technologies have been developed such as microneedles [4, 5]. Microneedles are structures up to 1 mm in length capable to penetrate the *stratum corneum*, the major skin barrier, in a pain-free way [4, 6], thereby delivering the antigen into the skin, a very immune competent organ populated with many antigen presenting cells. This may lead to antigen dose-sparing [4, 7] compared to the conventional routes of administration. Dissolving microneedles (dMNs) are a microneedle type that dissolve in the skin upon insertion thereby releasing the encapsulated vaccine [4]. Their dissolution in the skin allows to avoid sharp needle waste left behind after use and thus infections due to the needle re-use or needle-stick injuries are not possible [8]. Furthermore, for vaccine in the solid state it may be possible to circumvent the need for a cold-chain to keep the antigen stable during storage and shipping [9].

Vaccines consist of attenuated organisms, inactivated pathogens and toxins or subunit antigens. While attenuated vaccines may revert to the virulent form, inactivated and subunit vaccines are safer but generally less immunogenic [3, 10]. Thus, to potentiate the immune response using safer vaccines, together with the optimal administration route, adjuvants can be used, aiming for increased immunogenicity or antigen dose-sparing [4, 10, 11].

However, adjuvants can have drawbacks such as adverse effects and they may affect vaccine stability [11]. A previous study revealed that repeated administration of fractional doses of inactivated polio vaccine by means of a hollow microneedle (hMN) can lead to superior IgG responses without the use of adjuvants [12].

In this study, we examined whether the immunogenicity of diphtheria toxoid (DT) can be influenced by repeated dermal administration in comparison with a single dose without or with the addition of adjuvants. In a previous study the effect of repeated antigen dosing was assessed by using hMN [12]. In the present research, it was investigated whether repeated dosing by using dMNs and hMN had a similar effect on the immune response. To select the optimal adjuvant, the vaccination was performed by using a hMN intradermally in mice. This allowed to avoid time consuming dMN fabrication for all adjuvants and to screen a quite wide adjuvant set and to perform a relatively fast selection of them to encapsulate in the dMNs. Based on these studies, two adjuvants were selected for a follow-up study in which intradermal administration of DT and the adjuvant was performed in a single-full dose or in repeated-fractional dosing using either a hMN or dMNs.

2. MATERIALS AND METHODS

2.1 Materials

Hyaluronan (sodium hyaluronate, HA, average Mw was 150 kDa) was purchased from Lifecore Biomedical (Chaska, MN, USA). Diphtheria toxoid (DT) (12.25 mg/ml in phosphate buffered saline (PBS) pH 7.4) and diphtheria toxin (0.001 Lf/ml) were kindly provided by Intravacc (Bilthoven, The Netherlands). CpG ODN 1826 was purchased from Oligo Factory (Holliston, MA). Aluminum phosphate ($AlPO_4$) was purchased from Brenntag (Ballerup, Denmark). Fetal bovine serum (FBS) and cholera toxin (vibrio cholera) were obtained from Sigma-Aldrich (Zwijndrecht, The Netherlands). Glucose solution, L-Glutamine (200 mM), penicillin-streptomycin (10000 U/ml), and sodium bicarbonate were obtained from (Thermo-Fisher Scientific, Waltham, MA). Polyinosinic-polycytidylic acid (poly(I:C)) (low molecular weight) was purchased from Invivogen (Toulouse, France). Sterile phosphate buffered saline (PBS, 163.9 mM Na^+, 140.3 mM Cl^-, 8.7 mM HPO_4^{2-}, 1.8 mM $H_2PO_4^-$, pH 7.4) was ordered from Braun (Oss, The Netherlands). 10 mM phosphate buffer (PB, 7.7 mM Na_2HPO_4, 2.3 mM NaH_2PO_4, pH 7.4) was prepared in the laboratory. All the chemicals used were of analytical grade and distilled water (18 MΩ/cm, Millipore Co.) was used for the preparation of all solutions.

2.2 Synthesis of boehmite and gibbsite

Nanoparticulate aluminum salts boehmite and gibbsite were synthesized as described previously [13, 14]. Aluminium-iso-propoxide (80 mM) and aluminum-sec-butoxide (80 mM) were mixed in HCl (90 mM) and stirred for 10 days. The solution was hydrothermally treated at 150°C (boehmite) or 85°C (gibbsite) for 36h. The suspensions were dialyzed against water, autoclaved and stored at room temperature.

2.3 Preparation of formulations for hollow microneedle injections

In order to select the most promising adjuvants, various DT-adjuvant formulations were tested (Table 1) using a hMN injection system. DT was mixed in a concentration of 36 µg/ml with i) CpG ODN (36 µg/ml) or poly(I:C) (36 µg/ml) or cholera toxin (100 µg/ml) in PBS (pH 7.4), ii) the aluminum-based nanoparticles (alumNPs) gibbsite or boehmite (36 µg/ml Al^{3+} or 360 µg/ml Al^{3+}) in a sucrose (250 mM) containing histidine buffer (50 mM, pH 7.5). For the positive control, DT in a concentration of 500 µg/ml was mixed with $AlPO_4$ in a concentration of 15 mg/ml (DT-$AlPO_4$) in PBS (pH 7.4). AlumNPs and DT-$AlPO_4$ were incubated under continuous stirring at room temperature for 3 h to allow the DT adsorption on alumNPs or $AlPO_4$.

2.4 DT adsorption on alumNPs and $AlPO_4$

To determine the adsorption of free DT to alumNPs or $AlPO_4$, after the adsorption procedure the samples were centrifuged for 60 minutes at 35,000 × g at 4 °C in an Avanti J-20 XP centrifuge (Beckman Coulter). The DT in the supernatant was quantified by measuring the intrinsic fluorescence intensity of DT (λ_{ex} 280 nm/ λ_{em} 320 nm). The adsorption efficiency of DT was calculated according to the following equation:

$$\text{Adsorption efficieny } \% = (1 - \frac{M_{DT\ in\ supernatant}}{M_{DT\ total}}) \times 100\ \% \qquad \text{(Eqn. 1)}$$

where $M_{DT\ in\ supernatant}$ represents the mass of DT in supernatant after centrifugation, and $M_{DT\ total}$ is the total mass of DT used.

2.5 Particles size and zeta potential determination

For DT-alumNPs (DT in concentration of 36 µg/ml, alumNPs in concentrations of 36 µg/ml Al^{3+} or 360 µg/ml Al^{3+}) the particle size, polydispersity index (PDI) and zeta potential were determined by dynamic light scattering (DLS) and laser doppler velocimetry (Nano ZS® zetasizer, Malvern Instruments, Worcestershire, U.K.). To resemble the conditions for hMN injection and dMN arrays fabrication, samples were respectively prepared in 50 mM histidine (pH 7.5) or in 10 mM PB (pH 7.4).

2.6 Labeling of diphtheria, hyaluronan and alumNPs

2.6.1 Labeling for confocal microscopy

DT was labelled with Alexa Fluor 647® dye (AF647) (Life Technologies, Eugene, OR, USA) (λ_{ex} 651 nm, λ_{em} 672 nm) (DT-AF647) according to the manufacturer's instructions. Hyaluronan was labelled with fluoresceinamine (FAM) (Sigma-Aldrich, St. Louis, MO, USA) (isomer I, λ_{ex} 496 nm, λ_{em} 520 nm) (HA-FAM) following the method described by de Belder and Wik [15]. Gibbsite was labelled with lumogallion (Gib-LMG) (TCI Europe N.V., Antwerp, Belgium) (λ_{ex} 493 nm, λ_{em} 600 nm) following the method described by Mile et al [16].

2.6.2 Labeling for infrared detection

DT deposition in *ex vivo*-mouse and -human skin was quantified by using DT labelled with IRDye 800CW (LI-COR, Lincoln, Nebraska USA) (λ_{ex} 774 nm, λ_{em} 789 nm). DT labelling was performed according to the manufacturer's instructions.

2.7 Fabrication of dissolving microneedle arrays

dMN arrays (4x4 needles) were prepared as previously described [17, 18]. Briefly, 10% (w/v) HA was dissolved in PB (10 mM, pH 7.4) and stored overnight. The next day, 0.3% (w/v) DT for the full dose dMNs or 0.1% (w/v) DT for the fractional dose dMNs was added to the HA solution. The referred DT percentage for the full and fractional dose were defined to theoretically deliver 0.36 µg and 0.12 µg of DT respectively. The percentage was mathematically defined related to a previous publication [17]. For adjuvanted dMNs, the adjuvant in a weight ratio 1:1 with DT was added. For the DT adjuvanted with alumNPs, the alumNPs and DT were incubated under continuous stirring at room temperature for 3 h to allow the DT adsorption on alumNPs. Thus, the DT-alumNPs were added to the HA solution.

A polydimethylsiloxane mold (PDMS, Sylgard 184, Dow Corning, Midland, MI, USA) consisting of single-array wells was made using a master template presenting solid silicon MN arrays [17]. The PDMS mold was used to pour the HA-DT solution in each well. After several vacuum cycles and centrifugation steps, the dMN arrays were dried at 37°C overnight. The next day, an antigen-free backplate was produced by pouring a mixture of vinylpolysiloxane base and catalyst (1:1 ratio) (Elite Double 32a Normal, Zhermack Group, Badia Polesine, Italy). Subsequently a two-component glue solution (Bison International B.V., Goes, The Netherlands) was poured onto each array and left curing. Finally, the arrays were removed from the PDMS mold, cut into individual arrays and stored at room temperature in a desiccator until use.

To perform confocal imaging, in preparing the dMN arrays 100% of the DT and gibbsite amount and 4.5% of the hyaluronan amount were replaced with their labelled counterparts (DT-AF647, Gib-LMG and HA-FAM respectively). To perform near-infrared imaging of DT in the skin, 36% of the full dose of DT and 100% of the fractional dose of DT was labelled (DT-IR800).

2.8 Human skin

Human abdomen skin was obtained from a local hospital within 24 hours after cosmetic surgery. After removal of the fat excess with a scalpel, the skin was placed in the -80°C freezer until use. Before use, the skin was thawed in a petri dish containing a wet tissue at 37°C for 1 h and stretched with pins on parafilm-covered styrofoam. The skin was cleaned with distilled water and 70% ethanol before the start of the experiment.

Fresh *ex vivo* human skin was used within 24 hours after cosmetic surgery. After manual removal of the fat excess, the skin was cleaned with Milli-Q and 70% ethanol and stretched with pins on parafilm-covered Styrofoam to be used.

2.9 Penetration of microneedles in *ex vivo* human skin

dMN arrays (n=3) were applied onto the skin by impact velocity, as described elsewhere [18], by using an impact insertion applicator with a constant velocity of 0.40 m/s (Leiden University - applicator with uPRAX controller version 0.3) and kept in the skin during 18 sec. Penetration efficiency (PE) was determined by trypan blue treatment of pierced skin, as previously described [19]. After removal of the *stratum corneum* by stripping the blue spots were visualized using a light microscope. The penetration efficiency per array was calculated as follows (Equation 2), in which 16 is the number of microneedles per array:

$$\text{Penetration efficiency} = \frac{\text{Number of blue spots}}{16} \times 100 \qquad \text{(Eqn. 2)}$$

2.10 Dissolution of microneedles in *ex vivo* human skin

dMNs arrays (n=3) were applied on the skin as previously described (section 2.9) and were kept by the applicator for 20 min in the skin. The microneedle length before and after dissolution was determined with a light microscope (Axioskop and Stemi 2000-C, Carl Zeiss Microscopy GmbH, Göttingen, Germany) equipped with a digital camera (Axiocam ICc 5, Carl Zeiss). The images were analysed by ZEN 2012 blue edition software (Carl Zeiss Microscopy GmbH). The dissolved MN volumes were calculated as reported previously [17].

2.11 Quantification of diphtheria delivered in *ex vivo* mouse and human skin

Full dose dMN arrays (n=3 per skin type) and fractional dose dMN arrays (n=3 per skin type) were inserted into mouse or human skin *ex vivo* and the dMNs remained in the skin for 20 min. After dMN array removal, the near-infrared fluorescence of the delivered DT-IR800 was measured in a Perkin-Elmer IVIS Lumina Series III *in vivo* imaging system (Waltham, MA, USA), by using a ICG bkg excitation filter and an ICG emission filter and acquisition time 4 s, F-stop 2, binning 4 and field of view of 12.5 cm. Perkin-Elmer Living Image software version 4.3.1.0 was used for image acquisition and analysis. Fluorescence data were processed using region of interest (ROI) analysis with background subtraction consisting of a control region of the skin.

A calibration curve was generated in mouse and human skin by intradermal microinjections of DT-IR800 of 62.5 - 1000 ng with an in house fabricated hMN injection system with uPRAX controller version 0.3 (Leiden University) as reported elsewhere [12, 20, 21].

2.12 Confocal laser scanning microscopy

Confocal laser scanning microscopy (CLSM) was performed with a Nikon TE-2000-e inverted microscope equipped with a C1 confocal unit. Nikon Plan Apo 10 × and 4 × objectives (with a numerical aperture of 0.20 and 0.45 and working distance of 15.7 and 4 respectively) were used respectively for microneedle and skin visualization. Nikon NIS Elements version 4.20.00 64-bit software was used for acquisition and analysis of scans.

For dMN visualization, fluoresceinamine (FAM) and lumogallion (LMG) were excited at 488 nm and Alexa Fluor 647 at 633 nm. The xy resolution was 1.55 µm/pixel.

For antigen and nanoparticle localization in the skin, fluorescently labelled dMNs were inserted into *ex vivo* fresh human skin for 20 minutes. After removal of the remaining dMN array, time-lapse microscopy using CLSM as described above was performed with the skin in order to visualize hyaluronan, gibbsite or DT respectively. Each 30 min, sequentially xy scans (xy resolution of 6.21 µm/pixel) were taken with a spatial resolution of 10 µm in z-direction (z-axis of 0.7 mm) over a time period of 5 h.

2.13 Immunization studies

Immunization studies were performed using female BALB/c mice (H2d), 8-11 weeks old (Charles River, Maastricht, The Netherlands). The studies were approved by the ethical committee on animal experiments of Leiden University (License number 14241). The mice were randomly assigned to groups of 8.

Immunizations were given at day 1 (prime immunization), day 22 (boost immunization) and day 43 (2nd boost immunization). Before each intradermal immunization, the mice were shaved on the left flank (approximately 4 cm^2). A blood sample was collected, serum was isolated and stored at -80°C. Prior to vaccination, mice were anesthetized by intraperitoneal injection of 150 mg/kg ketamine and 10 mg/kg xylazine. At day 63, all mice were sacrificed and serum was collected.

2.13.1 Part I: adjuvant screening

The effect of adjuvants on the immunogenicity of dermally injected DT was assessed using hMN injection (Table 1). The inner diameter of the hMN was approximately of 150 µm and the length of the microneedle tip of approximately 120 µm. Injected volume was 10 µl at a controlled depth of 120 µm by using a specifically designed hMN injection system with uPRAX controller version 0.3 (Leiden University) [21]. Negative and positive controls included respectively intradermal injection of PBS by hMN and 100 µl subcutaneous injection of 5 µg DT and 150 µg $AlPO_4$ with a conventional 26G needle.

Table 1. Immunization study parameters for adjuvant screening. The dose of DT and adjuvant is provided together with the immunization route. Two ratios of DT and alumNPs were used.

Immunization route	**Intradermal by hollow microneedle**								**Subcutaneous**	
Group name[*)]	DT	DT-CT	DT-PI	DT-CpG ODN	DT-Gib		DT-Boe		PBS	DT- $AlPO_4$ sc
					1:1	1:10	1:1	1:10		
DT dose (µg)	0.36								-	5
Adjuvant dose (µg)	-	1	0.36		0.36[**)]	3.6 [**)]	0.36 [**)]	3.6 [**)]	-	150

[*)] DT, diphtheria toxoid; CT, cholera toxin; PI, poly(I:C); Gib, gibbsite; Boe, boehmite; $AlPO_4$, aluminum phosphate, [**)] Al^{3+} concentration.

2.13.2 Part II: single-full dose vs repeated-fractional doses

The effects of DT administration, with and without adjuvant, in repeated-fractional doses (RFrD) were investigated and compared to a single-full dose (SFD) injection (100% dose). The RFrD consisted of administration, in 3 consecutive days, of 1/3rd of the SFD of DT(-adjuvant) (3 x 33% doses). Intradermal vaccination in mice was performed using hMN (10 µl at a depth of 120 µm) and dMNs. Details of the formulations are reported in Table 2. PBS and DT- $AlPO_4$ groups were used as negative and positive control, respectively. An additional positive control of subcutaneous injection of 100 µl of 0.36 µg DT and 0.36 µg poly(I:C) was included.

Table 2. Immunization study parameters for administration kinetics investigation. The administration is in SFD (100%) or in 3 RFrD (3 x 33%).

Formulation	Formulation dose administration schedule	DT dose*) per array/injection (μg)
Intradermal administration: dissolving microneedles		
DT DT-Gib DT-PI E/E/DT**)	SFD	0.36
DT DT-Gib DT-PI	RFrD	0.12
Intradermal injection: hollow microneedles		
DT PBS/PBS/DT**)	SFD	0.36
DT	RFrD	0.12
PBS	-	-
Subcutaneous injection (conventional 26G needle)		
DT-PI	SFD	0.36
DT-$AlPO_4$	SFD	5

*) the DT and adjuvant dose are equal except for the subcutaneous injection with $AlPO_4$, in which 5 μg of DT and 150 μg $AlPO_4$ has been added in the formulation; **) application of an empty dMN array or injection of PBS on 2 consecutive days and DT administration in SFD on day 3. Abbreviations are DT, diphtheria toxoid; Gib, gibbsite; PI, poly(I:C); $AlPO_4$, aluminum phosphate; E, empty dMN array.

2.14 Determination of DT-specific serum IgG titers and diphtheria toxin-neutralizing antibody titers

DT-specific total IgG, IgG1 and IgG2a titers in serum were determined by ELISA as described previously [22]. Plates were coated with 140 ng DT per well and incubated overnight at 4 °C. After blocking with BSA (Sigma-Aldrich, Zwijndrecht, The Netherlands), sera samples were added in a three-fold serial dilution and the plates were incubated at 37 °C for 2 h. Detection of antibodies was performed with horseradish peroxidase-conjugated goat-anti-mouse IgG, IgG1 or IgG2a (Southern Biotech, Birmingham, AL) (1:5000 dilution) using 1-stepTM ultra 3,3',5,5'-tetramethylbenzidine (TMB) (Thermo-Fisher Scientific, Waltham, MA) as substrate. The reaction was stopped with 2 M sulfuric acid (JT Baker, Deventer, The Netherlands). Absorbance was measured at 450 nm. Antibody titers were expressed as the log10 value of the serum dilution at the mid-point of the S-shaped absorbance-dilution curve.

Toxin neutralizing capacity of antisera was measured in a Vero cell assay [23]. After complement inactivation by heating at 56 °C for 45 min, appropriate two-fold serial dilutions of serum samples were prepared in M199 medium (Sigma-Aldrich, Zwijndrecht, The Netherlands) (supplemented with 5% FBS (Sigma-Aldrich, Zwijndrecht, The Netherlands), 1 g/l glucose, 1.6 mM L-glutamine, 1.7 g/l sodium bicarbonate and 100 U/ml penicillin-streptomycin) and were applied to 96-well plates. Subsequently, 50 µl/well 0.001 Lf/ml diphtheria toxin diluted in complete culture medium was added and the plates were incubated at 37°C and 5% CO_2 for 2 h for toxin neutralization. Subsequently, 50 µl/well suspension of Vero cells were added (12,500 cells/well) and incubated at 37 °C in 5% CO_2 for 6 days. The number of wells containing viable Vero cells was determined by microscopy. The neutralizing antibody titers were expressed as the log2 value of the highest serum dilution that was still capable of protecting the Vero cells from the challenge of diphtheria toxin.

2.15 Statistical analysis

Data from antibody titers and neutralizing antibody titers were analyzed by one way ANOVA with Bonferroni post-test by using GraphPad Prism software (version 5.02). A $p < 0.05$ was considered to be significant.

3 RESULTS

3.1 Size and zeta potential of DT-alumNPs and adsorption efficiency of DT to alumNPs and to $AlPO_4$

DT-Gibbsite and DT-Boehmite were characterized in terms of particle size, polydispersity index (PDI) and zeta potential. DT-alumNPs were in the µm range, i.e. outside the measuring range of the DLS equipment, regardless the buffer composition (data not shown).

The effect of the type of particle on the zeta potential was examined. In histidine buffer, boehmite resulted in a positive surface charge, while gibbsite showed a negative zeta potential at the same concentration. When increasing the particle concentration the zeta potential became less negative for the boehmite and became positive for the gibbsite. The effect of the addition of DT on the zeta potential was also examined. It was observed that i) addition of DT to the alumNPs formulation resulted in a lower zeta potential than alumNPs only and ii) increasing the DT:alumNPs ratio from 1:1 to 1:10 by increasing the alumNP concentration resulted in a higher zeta potential, indicating a relative lower level of negatively charged DT on their surface compared with the slightly positively charged alumNPs (Table 3). No significant changes in zeta potential were observed within the first 24 h of storage (Table 3). The alumNPs in PB showed a more negative zeta potential than in histidine buffer.

The adsorption efficiency of DT on the alumNPs and $AlPO_4$ at 3 h after mixing was measured (Table 3). In solutions with DT : alumNPs 1:10 ratio more than 80% DT was adsorbed to the alumNPs. For a DT : alumNPs 1:1 ratio the DT adsorption on the alumNPs was less than 40%. This was also observed for the $AlPO_4$ particles. This indicated that at equal weight ratios the alumNP surface became saturated with DT.

Table 3. Zeta potential of DT-alumNPs and percentages of DT adsorption on alumNPs and $AlPO_4$ (n = 3). Data are average ± SEM.

		Time (h)			
		0	3	24	
Formulation	**Buffer**	**Zeta Potential (mV)**			**Adsorption efficiency (%)**
Gibbsite*)	PB	-24.7 ± 0.4	-	-	-
DT-Gibbsite*) 1:1		-32.6 ± 0.5	-32.8 ± 0.3	-32.1 ± 0.3	27.1 ± 0.5
Gibbsite*)	Histidine	-0.9 ± 0.3	-	-	-
DT-Gibbsite*) 1:1		-27.1 ± 0.1	-27.0 ± 0.2	-26.7 ± 0.2	11.4 ± 1.0
Gibbsite**)		17.6 ± 0.3	-	-	-
DT-Gibbsite**) 1:10		-22.8 ± 0.3	-22.5 ± 0.2	-19.0 ± 0.6	81.3 ± 0.1
Boehmite*)		3.4 ± 0.4	-	-	-
DT-Boehmite*) 1:1		-23.8 ± 0.2	-23.2 ± 0.2	-25.7 ± 0.1	25.5 ± 0.4
Boehmite**)		13.9 ± 0.5	-	-	-
DT-Boehmite**) 1:10		-15.4 ± 0.6	-8.5 ± 0.2	-4.7 ± 0.5	83.2 ± 0.1
DT-$AlPO_4$ 1:30	PBS	-	-	-	38.7 ± 0.3

*) 36 µg/ml Al^{3+}, **) 360 µg/ml Al^{3+}

3.2 Immunization study for adjuvant screening

In an immunization study using a hMN several adjuvants were screened on their efficiency to potentiate the immune response of DT. The selected adjuvants were CpG ODN, Poly(I:C), cholera toxin, gibbsite and boehmite (the latter two in DT : alumNPs ratios of 1:1 and 1:10).

After the prime, the groups DT-Gib 1:1 and DT-Boe 1:10 induced higher IgG titers than the DT group (Figure 1 A). The DT-Boe 1:10 group showed even a comparable response to the positive control DT-$AlPO_4$ (Figure 1 A).

At day 42, DT-specific total IgG titers increased further for all formulations (Figure 1 B). However, no significant adjuvant effect was observed in comparison with the DT control group (Figure 1 B). The DT-CT group had a comparable IgG response to the positive control DT-$AlPO_4$.

At day 63 (Figure 1 C), the response of all the groups was very close to the response of positive control DT-$AlPO_4$, despite a 15 fold lower dose (Figure 1 C). However, the addition of different adjuvants did not enhance further the response evoked by DT after three vaccinations (Figure 1 C).

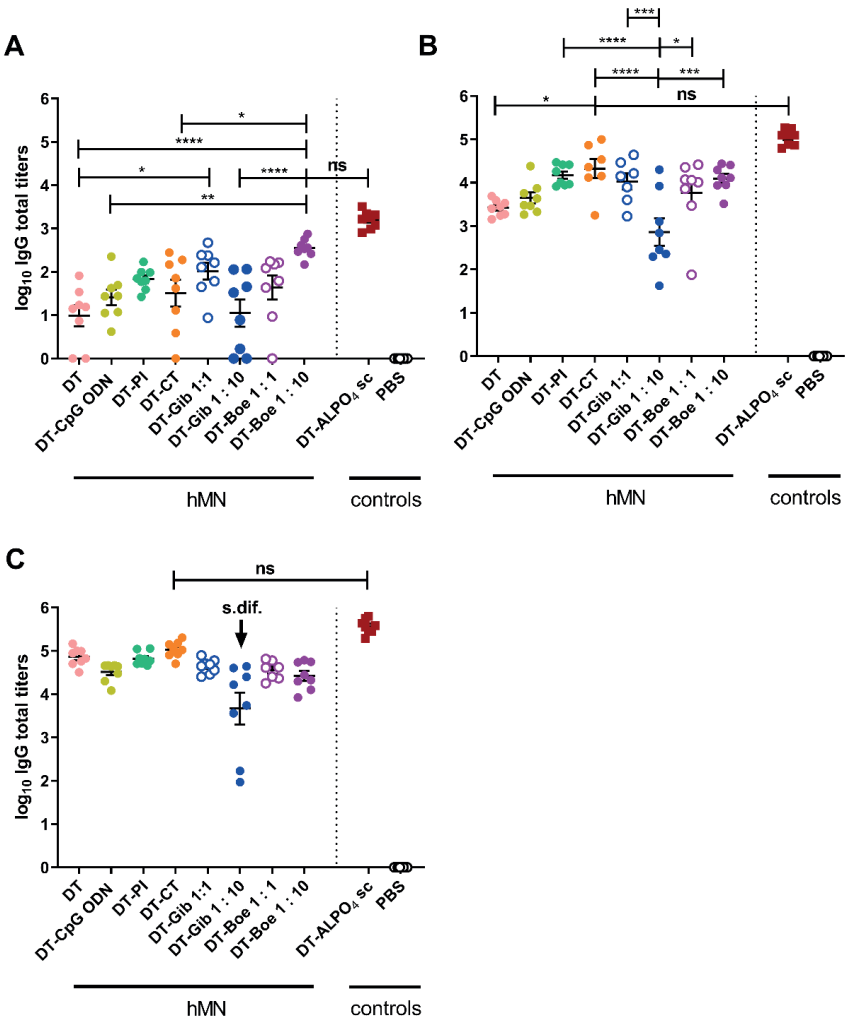

Figure 1. DT-specific total IgG titers on day 21 **(A)**, 42 **(B)** and 63 **(C)**. After each vaccination, the $AlPO_4$ was significantly different from each other group except the no significant (ns) group reported. After 63 days, the titers in the DT-Gib 1:10 group was significantly lower (s.dif.) compared to the titers in all the other groups. Bars represent mean ± SEM, n = 8. *p < 0.05, **p < 0.01, ***p < 0.001 and ****p < 0.0001. DT dose was 0.36 µg except DT-$AlPO_4$ sc: 5 µg. hMN, hollow microneedle; DT, diphtheria toxoid; PI, poly(I:C); CT, cholera toxin; Gib, gibbsite; Boe, boehmite; $AlPO_4$, aluminum phosphate.

Besides the IgG total response, the IgG1 and IgG2a responses were also measured. IgG1 and IgG2a ratios were not dependent on adjuvant type (Supplementary material, Figure S1) (p>0.05). This indicates that the Th2/Th1 balance was not influenced by the adjuvants.

The functionality of the antibody response was investigated by determining toxin neutralizing antibody titers in serum on day 63. The positive control DT-$ALPO_4$ showed higher levels of toxin-neutralizing antibodies than all other groups ($p<0.05$) (Figure 2). Overall, the addition of an adjuvant to DT did not improve the functional response. Similarly to the IgG total titers, DT-Gibbsite 1:10 was less immunogenic as compared to plain DT.

Based on neutralizing antibody results and the primary response, poly(I:C) and gibbsite (the formulation in 1:1 ratio with DT) were selected as adjuvants for the studies using dMNs.

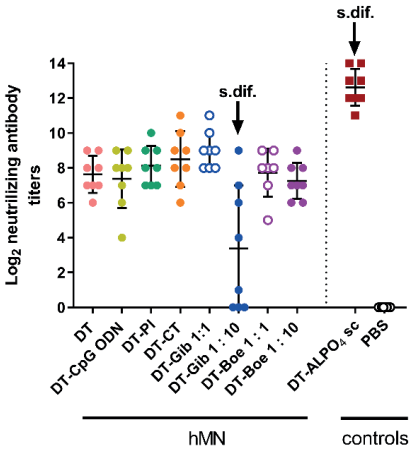

Figure 2. DT-neutralizing antibody titers. Results are shown for serum collected on day 63. The titers in the DT-Gib 1:10 group and the DT-$AlPO_4$ group were, respectively, significantly lower or higher (s.dif.) from the titers in all the other groups. Bars represent mean ± SEM, n = 8. hMN, hollow microneedle; DT, diphtheria toxoid; PI, poly(I:C); CT, cholera toxin; Gib, gibbsite; Boe, boehmite; $AlPO_4$, aluminum phosphate.

3.3 Dissolving microneedle: characterization and interaction with the skin

dMN arrays were prepared with DT in absence or presence of the selected adjuvant. Very sharp dMNs containing either DT, DT-PI or DT-Gib could be prepared (Figure 3) in a reproducible manner. The DT content (full dose or fractional dose) did not affect the shape either (Figure 3 and data not shown).

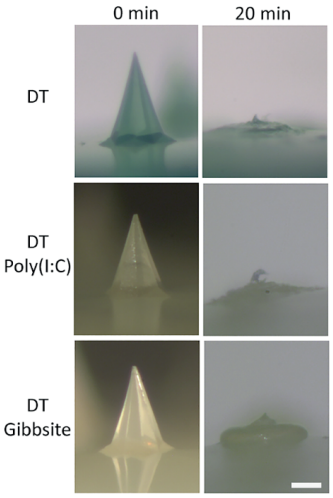

Figure 3. Brightfield microscope images (5x) of microneedles with DT, DT-PI and DT-Gib full dose content before application on the skin (0 min) and after 20 minutes dissolution into *ex vivo* human skin. Scale bar 100 µm.

Hyaluronan, DT and gibbsite were uniformly distributed within the dMN as investigated with confocal 3D imaging using fluorescently labelled components (Figure 4).

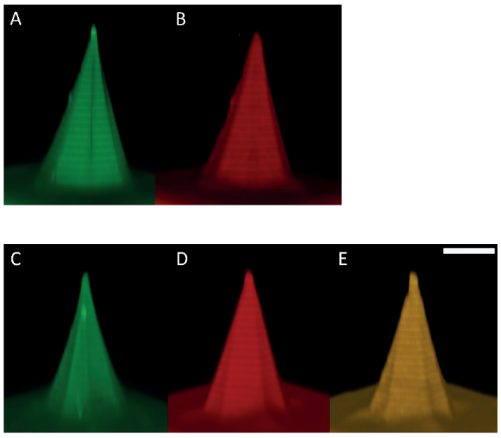

Figure 4. CLSM 3D images of the distribution of fluorescently labelled HA **(A)** and DT **(B)** in the hyaluronan-based dMNs containing DT; Fluorescently labelled HA **(C)**, DT **(D)** and Gib **(E)** in hyaluronan-based dMNs containing DT adsorbed gibbsite nanoparticles. Both dMNs **(A-B and C-E)** contained a full dose of DT or DT-Gib. Scale bar 100 µm.

dMN arrays prepared from full dose of either DT, DT-PI or DT-Gib were applied on *ex vivo* human skin. After withdrawal and application of trypan blue, the number of blue spots were determined and the penetration efficiency and the standard deviation were calculated being respectively 95.8 ± 7.2%, 89.6 ± 9.5% and 100.0 ± 0.0%, respectively (n = 3).

As shown in Figure 3, dMNs with DT or DT-PI incorporated dissolved completely in the skin within 20 min (100 ± 0% dissolved MN volume, mean ± sd), the dMNs with DT-Gib incorporated resulted in some dMN leftover (approximately 91 ± 1% dissolved volume, mean ± sd).

After 20 min microneedle dissolution in fresh human skin and withdrawal of the remaining dMN array, the hyaluronan, DT and gibbsite were visualized in the skin by CLSM during 5 hours each 30 minutes as function of depth parallel to the skin surface (Figure 5, only 0, 3 and 5 h time points are shown). All components were deposited and co-localized in the epidermis and top layers of the dermis. Furthermore, the delivered antigen without or with gibbsite remained at the site of administration for at least 5 h, whereas HA is mostly diffused away after 3 h or less.

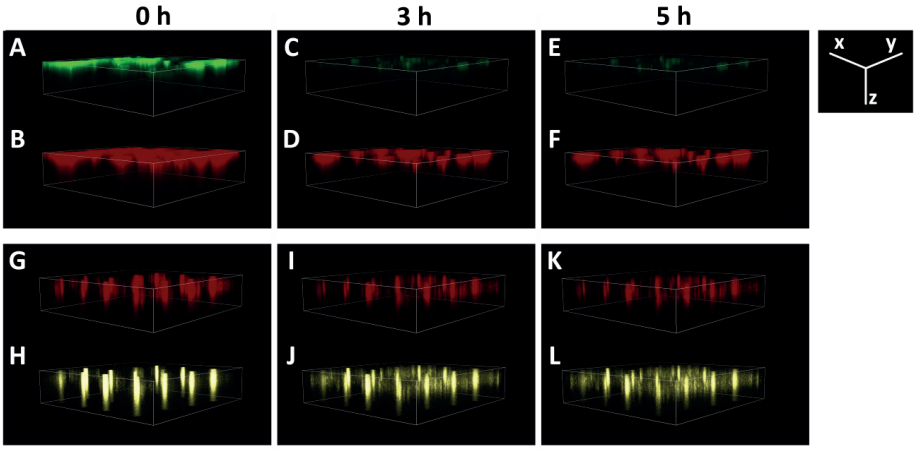

Figure 5. CLSM 3D images of HA (green), DT (red) and Gib (yellow) localization into *ex vivo* human (fresh) skin after dMN arrays application for 20 min. Deposited HA **(A, C, E)** and DT **(B, D, F)** fluorescently labelled (HA-FAM and DT-AF647) into the skin after dissolution of hyaluronan dMNs loaded with DT; deposited DT **(G, I, K)** and gibbsite **(H, J, L)** fluorescently labelled (DT-AF647 and Gib-LMG) into the skin after dissolution of hyaluronan dMNs loaded with DT and gibbsite. Images related to time 0 h **(A, B, G, H)**, 3 h **(C, D, I, J)** and 5 h **(E, F, K, L)** are shown. Time 0 h refers to the beginning of the detection, starting after the dMN dissolution of 20 min and removal of the dMN array. The location of the skin surface is the xy area on top of the z-axis representing the depth of imaging (0.7 mm).

Finally, the amount of DT delivered into the skin after dMN array application using infrared labelled DT was determined. After 20 min of application in the skin, the dMNs containing a full or 1/3 dose of DT delivered respectively 0.32 ± 0.02 µg and 0.13 ± 0.04 µg of DT in *ex vivo* human skin and 0.35 ± 0.03 µg and 0.10 ± 0.01 µg of DT in *ex vivo* mouse skin (mean ± sd, n = 3).

3.4 dMN arrays and hMNs: single-full dose vs. repeated-fractional dose

The aim of this study was to compare RFrD with SFD administration of DT with or without adjuvant using dMN arrays and a hMN keeping the total dose of DT and antigen approximately the same.

Following prime vaccination by a hMN, IgG titers after DT RFrD were higher than DT SFD (Figure 6 A). To determine whether MN piercing itself has an effect on the immune response, a hMN group (PBS/PBS/DT SFD) consisting of two consecutive days of PBS injection and a third day of SFD DT injection was included. As the IgG titers were higher than that of the SFD injection, microneedle piercing as such seems to enhance the immune response.

Prime administration of DT by dMNs gave higher IgG responses than hMN injection (Figure 6 A). DT RFrD by dMNs did not significantly increase the IgG levels compared to DT SFD by dMNs, although there is a trend of a higher response and after RFrD there is less variation in the response. Additionally, the application of empty dMN arrays in the first two days and the SFD administration of the DT on the third day (E/E/DT SFD) showed a comparable IgG response as RFrD. The encapsulation of an adjuvant (poly(I:C) or gibbsite) together with DT in the dMNs, did not increase the DT-specific total IgG response when delivered as SFD or RFrD compared to the absence of an adjuvant. Finally, the administration of DT by dMNs gave a higher response than the control of DT-poly(I:C) injected subcutaneously and a response comparable to the positive control, DT-$AlPO_4$ sc, with a 15 times higher DT dose. Conversely, the hMN groups showed comparable response to the control of DT-PI sc and a significantly lower response than the positive control DT-$AlPO_4$ sc.

After the first boost, DT-specific total IgG titers increased (Figure 6 B) but the differences between the groups were similar as after the prime with a few changes. DT RFrD by dMNs was comparable to DT RFrD using hMN but still higher than PBS/PBS/DT SFD hMN group. Furthermore, the positive controls DT-PI and DT-$AlPO_4$ subcutaneously injected were comparable to all hMN and dMNs groups except to DT SFD hMN and DT SFD hMN and PBS/PBS/DT SFD hMN groups, respectively, which showed a significant lower response.

After the second boost (Figure 6 C) the titers of most groups further increased, although slightly. Apparently a plateau in the immune response was reached. After this second boost, for the first time the DT RFrD dMNs group developed a higher response than E/E/DT SFD dMNs.

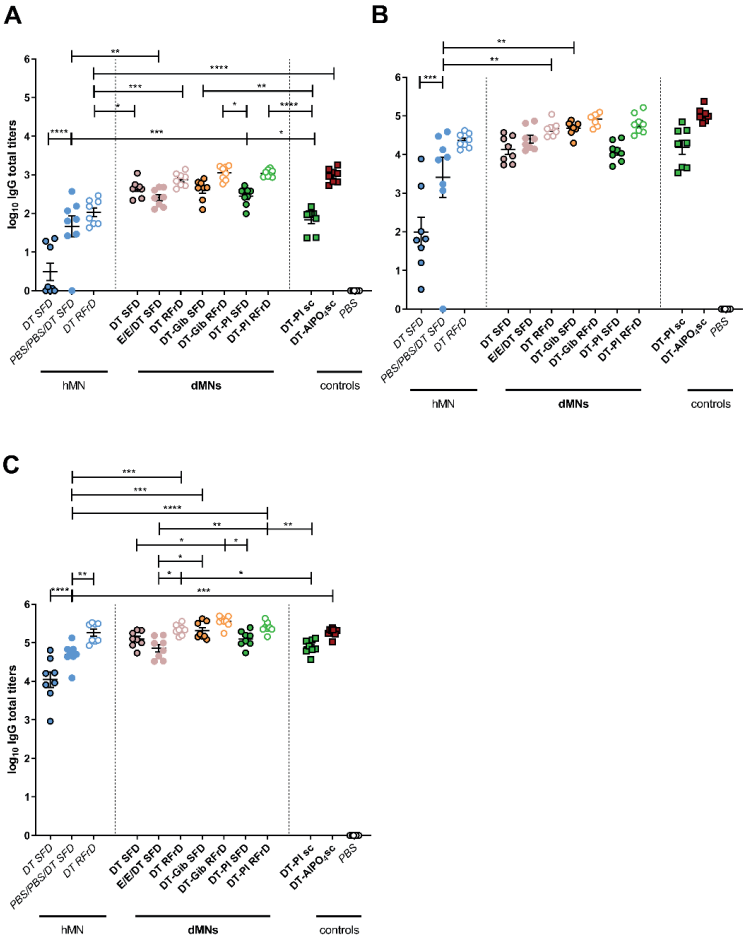

Figure 6. DT-specific total IgG antibody titers measured in BALB/c mice on day 21 **(A)**, day 42 **(B)** and day 63 **(C)**. Bars represent mean ± SEM, n = 8. *p < 0.05, **p < 0.01, ***p < 0.001, ****p < 0.0001. SFD, single-full dose; RFrD, repeated-fractional dose; dMNs, dissolving microneedles; hMN, hollow microneedle; DT, diphtheria toxoid; PI, poly(I:C); Gib, gibbsite; E, empty dMNs; $AlPO_4$, aluminum phosphate.

The IgG1/IgG2a ratios are depicted in Figure S2 in Supplementary material. DT vaccination by dMNs and addition of gibbsite or poly(I:C) as adjuvant modestly changed the IgG1/IgG2a ratio, shifting the balance slightly to Th1.

High levels of toxin-neutralizing antibodies were induced after vaccination by means of dMNs, regardless the dosing modality or the presence of an adjuvant, and by DT RFrD by

hMN (Figure 7). No adjuvant effect was observed after addition of PI in dMNs (DT SFD dMNs gave a similar response compared to DT-PI SFD dMNs and DT-PI SFD sc), but DT-PI RFrD dMNs resulted higher in response compared to DT-PI SFD dMNs and DT-PI SFD sc. In this case, the dosing modality made a difference in protection against the toxin, resulting a RFrD of DT-PI in a much higher toxin neutralization.

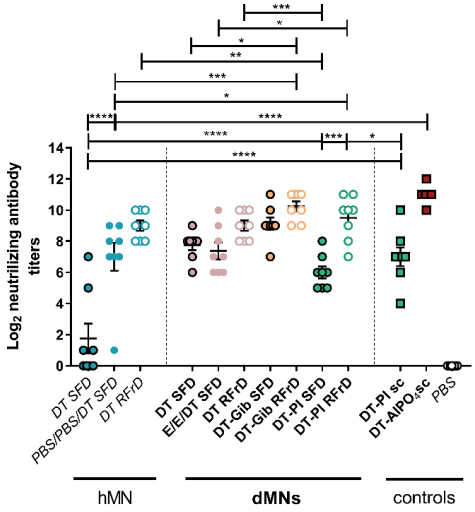

Figure 7. DT-neutralizing antibody titers. Results are shown for serum collected on day 63. Bars represent mean ± SEM, n = 8. *p < 0.05, **p < 0.01, ***p < 0.001, ****p < 0.0001. SFD, single-full dose; RFrD, repeated-fractional dose; dMNs, dissolving microneedles; hMN, hollow microneedle; DT, diphtheria toxoid; PI, poly(I:C); Gib, gibbsite; E, empty dMNs; $AlPO_4$, aluminum phosphate.

4. DISCUSSION

Repeated-fractional doses effect

The aim of this study was to obtain insight in whether dermal vaccination by RFrD of DT enhances the specific IgG response compared to that after SFD antigen dermal administration. The present study corroborated existing data [12, 24] by showing a superior response by RFrD compared to SFD of antigen after vaccination by hMN. In the present study less consecutive days of administration were used as in the previous studies: 33% in each consecutive day during 3 days vs 4, 7 and 8 days in the previous studies. Furthermore, low responders seemed to benefit more from the RFrD regime and it was demonstrated that consecutive skin piercing by hMN (PBS/PBS/DT SFD) could enhance the immune response compared to a DT SFD only by hMN. Piercing of the skin may cause some cell death or other local damage resulting in the release of damage-associated molecular patterns (DAMPs) and subsequent attraction of antigen presenting cells to the immunization area [25]. However,

application of empty dMN arrays (E/E/DT SFD), inducing an even higher number of piercings in the skin compared to a hMN (16 dMNs per array vs 1 hMN) and applied by a 20 minutes pressure on the skin potentially leading to skin inflammation [25, 26]. This did not enhance the response further compared to a SFD antigen administration by dMNs. This may be explained by a maximal level of immunity reached after prime for the E/E/DT SFD group due to the skin piercing by the first empty array application inducing release of DAMPs and then an immune response with no additional further effect after application of the other empty and then DT loaded dMN arrays.

dMNs vs a hMN

Vaccination by means of dMNs led to significantly higher response than by hMN, as already reported in our previous study [17], showing a faster increase in DT-specific IgG responses already after the first immunization. This can be related to several factors. First, the use of different MN types: a hMN injects the vaccine at a specific intradermal depth point (120 µm) while the longer dMNs (300 µm) release the antigen at various skin depths simultaneously possibly reaching a higher number of immune cells and involving different immune cell populations [27], although in literature no difference in the immune response is reported when comparing different injection depths [20]. Second, the number of needles piercing the skin (16 dMNs vs 1 hMN) and the pressure applied on the skin (20 minutes for the dMN array application and no pressure for the hMN) potentially causing inflammation and thus more release of DAMPs in a larger region, facilitating attraction of antigen presenting cells. Third, the presence of low molecular weight species of HA. Although high MW HA is considered immunologically inert, low molecular weight HA fragments, potentially present in the dMNs or generated *in vivo*, can elicit various proinflammatory responses leading to innate immune activation [28, 29], although this is not observed in recent studies in our group [30] and in literature [31]. Fourth, the prolonged exposure of the antigen during dMN dissolution to relevant immune cells may enhance the response [32]. Fifth, the presence of low responding and no-responding mice after prime vaccination in SFD by hMN: in a previous study [22] and in the adjuvants screening of the present study, the titers after DT vaccination by hMN resulted in an overall higher response being closer to the positive control DT-$AlPO_4$ than in the SFD vs RFrD immunization study.

Adjuvants vs repeated-fractional dosing by dMNs

Antigen dose sparing can be achieved with the use of adjuvants [10, 23]. Besides adjuvants (CpG, PI and CT) commonly used for experimental dermal vaccination [1, 4, 23], aluminum-based NPs (alumNPs), so far tested only for subcutaneous or intramuscular administration [10, 33, 34], were included for intradermal vaccination.

The selection, in the first immunization study by hMN, of the optimal adjuvants for DT vaccination by dMNs led to the choice of poly(I:C) and gibbsite. Poly(I:C) gave a more robust response after primary immunization, similar to CT, than other adjuvants and it has a better

feasibility for human vaccination than CT. The selection of gibbsite (in ratio 1:1 with DT) was based on the following considerations: i) its higher response among the DT adjuvanted with alumNPs and ii) dermal injection of gibbsite, as of boehmite too, did not induce any palpable persistent intradermal injection-site nodules in mice, as previously observed after intradermal injection of classical aluminum preparations [35].

The addition of adjuvants for intradermal vaccination by both hMN and dMNs did not enhance the IgG total levels further compared to unadjuvanted antigen indicating that the response reached already a plateau and any extra did not lead to a higher response. However, vaccination by dMNs, in the presence of poly(I:C) or gibbsite, shifted the Th2/Th1 balance to Th1. This was not observed using hMNs. This change in response may be related to the depot created in the skin after dMN dissolution leading to a sustained release of antigen and adjuvant [32].

In our study, similarly potent DT-specific IgG responses were observed upon intradermal vaccination by dMNs of SFD, RFrD and adjuvanted DT. This demonstrates that by using dMNs the immune response can be enhanced and the use of an adjuvant or prolonged antigen delivery by fractional dosing can be avoided, at least for potent antigens. An adjuvant-free vaccine would then avoid side-effects and potential stability problems related to the presence of the adjuvant [11, 36].

However, results from neutralizing antibody assay indicated a higher protection against diphtheria toxin for adjuvanted-DT RFrD dMNs compared to unadjuvanted DT in dMNs, hMN groups and even conventional injection of DT-PI. This may be related to a prolonged exposure of the antigen during and after dMN dissolution to relevant immune cells involved in the humoral protection as mentioned above.

Overall these observations lead to the conclusion that the combination of RFrD and adjuvant in dMNs, but not their separated use, can be very efficient in respect to the antibody response and the neutralization of the diphtheria toxin effect.

Finally, Joice et al [37] reported how extended-delivery vaccination by means of dMNs enables a single vaccination to generate immune responses equivalent to a two-dose vaccination regimen for vaccines as IPV, tetanus toxoid and influenza but the same extended-delivery vaccination does not enhance immune response to the live-attenuated measles vaccine. This demonstrates that RFrD of the antigen can lead to a superior immune response than SFD depending on the antigen type.

dMNs vs conventional subcutaneous injections

This study focused on minimally-invasive delivery for DT immunization by dMNs and it has been shown that vaccination by dMNs loading unadjuvanted DT led to comparable responses already after prime immunization as compared to invasive subcutaneous injections of DT-$AlPO_4$ with almost 15 and 415 times higher DT and adjuvant doses

respectively. These results corroborated existing data in literature where a comparable or even higher response was obtained after vaccination by dMNs than conventional subcutaneous injection [27, 38-41] and similar response was shown after vaccination with hMN in comparison with the above mentioned positive control [1, 22]. Higher IgG responses after prime and comparable responses after the two boost immunizations demonstrate the efficiency of a dermal vaccination by dMNs compared to subcutaneous injection of adjuvanted-DT (DT-PI sc).

Characterization of the alumNPs

Fabrication of dMN arrays and dMN interaction with the skin, regardless the formulation, was successful as previously demonstrated [17]. However, dissolution of DT-Gib was not complete after 20 minutes. This may be related to the particle aggregation observed in the alumNPs characterization studies. Aggregation is likely due to the pH, as the alumNPs are stable at pH<6 and aggregate above this value (H. Vrieling et al, manuscript in preparation).

Boehmite and gibbsite were characterized in the transmission electron microscope for their shape and size resulting in nm range [42, 43]. In the present study their size resulted in the µm range using dynamic light scattering (data not shown). This suggests that particle aggregation occurred. Besides the presence of DT and the concentration of alumNPs, the buffer composition also had a role on the zeta potential: PB lowered the zeta potential more than the histidine buffer. A possible explanation can be found in the phosphate groups from PB exchanging with hydroxyl groups of alumNPs so that a mixture of aluminum oxyhydroxide and aluminum phosphate is obtained.

5. CONCLUSION

In conclusion, when using hMN a delivery of the antigen over multiple days can enhance the immune response more than a SFD delivery. The SFD vaccination by dMNs can enhance a much higher response than hMN, however fractional delivery administration by using dMNs does not lead to a superior response. Moreover, dMNs demonstrate no further increase in response by co-encapsulation of the adjuvant and a comparable or even higher response than, respectively, the current benchmarks: $AlPO_4$ adsorbed DT and DT-PI administered subcutaneously. These findings demonstrate the potential of dMNs as vaccine delivery device addressing to a SFD administration of an adjuvant-free vaccine to have a fast and high functional response.

Acknowledgements

We thank Amy Kogelman from Intravacc for her help with the neutralizing antibody assay.

REFERENCES

1. G. Du, M. Leone, S. Romeijn, G. Kersten, W. Jiskoot, J.A. Bouwstra, Immunogenicity of diphtheria toxoid and poly(I:C) loaded cationic liposomes after hollow microneedle-mediated intradermal injection in mice, Int J Pharm, 547 (2018) 250-257.
2. H. Jiang, Q. Wang, X. Sun, Lymph node targeting strategies to improve vaccination efficacy, J Control Release, 267 (2017) 47-56.
3. L.J. Peek, C.R. Middaugh, C. Berkland, Nanotechnology in vaccine delivery, Adv Drug Deliv Rev, 60 (2008) 915-928.
4. M. Leone, J. Monkare, J.A. Bouwstra, G. Kersten, Dissolving Microneedle Patches for Dermal Vaccination, Pharm Res, (2017).
5. E. Larraneta, M.T. McCrudden, A.J. Courtenay, R.F. Donnelly, Microneedles: A New Frontier in Nanomedicine Delivery, Pharm Res, 33 (2016) 1055-1073.
6. K. van der Maaden, W. Jiskoot, J. Bouwstra, Microneedle technologies for (trans)dermal drug and vaccine delivery, J Control Release, 161 (2012) 645-655.
7. N. Li, L.H. Peng, X. Chen, S. Nakagawa, J.Q. Gao, Transcutaneous vaccines: Novel advances in technology and delivery for overcoming the barriers, Vaccine, 29 (2011) 6179-6190.
8. Y.C. Kim, J.H. Park, M.R. Prausnitz, Microneedles for drug and vaccine delivery, Adv Drug Deliv Rev, 64 (2012) 1547-1568.
9. H.S. Gill, M.R. Prausnitz, Coated microneedles for transdermal delivery, J Control Release, 117 (2007) 227-237.
10. S.G. Reed, M.T. Orr, C.B. Fox, Key roles of adjuvants in modern vaccines, Nat Med, 19 (2013) 1597-1608.
11. O.S. Kumru, S.B. Joshi, D.E. Smith, C.R. Middaugh, T. Prusik, D.B. Volkin, Vaccine instability in the cold chain: mechanisms, analysis and formulation strategies, Biologicals, 42 (2014) 237-259.
12. P. Schipper, K. van der Maaden, S. Romeijn, C. Oomens, G. Kersten, W. Jiskoot, J. Bouwstra, Repeated fractional intradermal dosing of an inactivated polio vaccine by a single hollow microneedle leads to superior immune responses, J Control Release, 242 (2016) 141-147.
13. P.A. Buining, C. Pathmamanoharan, J.B.H. Jansen, H.N.W. Lekkerkerker, Preparation of Colloidal Boehmite Needles by Hydrothermal Treatment of Aluminum Alkoxide Precursors, J Am Ceram Soc, 74 (1991) 1303-1307.
14. A.M. Wierenga, T.A.J. Lenstra, A.P. Philipse, Aqueous dispersions of colloidal gibbsite platelets: synthesis, characterisation and intrinsic viscosity measurements, Colloid Surface A, 134 (1998) 359-371.
15. A.N. de Belder, K.O. Wik, Preparation and properties of fluorescein-labelled hyaluronate, Carbohydr Res, 44 (1975) 251-257.
16. I. Mile, A. Svensson, A. Darabi, M. Mold, P. Siesjo, H. Eriksson, Al adjuvants can be tracked in viable cells by lumogallion staining, J Immunol Methods, 422 (2015) 87-94.
17. M. Leone, M.I. Priester, S. Romeijn, M.R. Nejadnik, J. Monkare, C. O'Mahony, W. Jiskoot, G. Kersten, J.A. Bouwstra, Hyaluronan-based dissolving microneedles with high antigen content for intradermal vaccination: Formulation, physicochemical characterization and immunogenicity assessment, Eur J Pharm Biopharm, 134 (2019) 49-59.
18. M. Leone, B.H. van Oorschot, M.R. Nejadnik, A. Bocchino, M. Rosato, G. Kersten, C. O'Mahony, J. Bouwstra, K. van der Maaden, Universal Applicator for Digitally-Controlled Pressing Force and Impact Velocity Insertion of Microneedles into Skin, Pharmaceutics, 10 (2018).
19. K. van der Maaden, E. Sekerdag, W. Jiskoot, J. Bouwstra, Impact-insertion applicator improves reliability of skin penetration by solid microneedle arrays, Aaps J, 16 (2014) 681-684.
20. P. Schipper, K. van der Maaden, S. Romeijn, C. Oomens, G. Kersten, W. Jiskoot, J. Bouwstra, Determination of Depth-Dependent Intradermal Immunogenicity of Adjuvanted Inactivated Polio Vaccine Delivered by Microinjections via Hollow Microneedles, Pharm Res, 33 (2016) 2269-2279.
21. K. van der Maaden, S.J. Trietsch, H. Kraan, E.M. Varypataki, S. Romeijn, R. Zwier, H.J. van der Linden, G. Kersten, T. Hankemeier, W. Jiskoot, J. Bouwstra, Novel hollow microneedle technology for depth-controlled

microinjection-mediated dermal vaccination: a study with polio vaccine in rats, Pharm Res, 31 (2014) 1846-1854.
22. P. Schipper, K. van der Maaden, V. Groeneveld, M. Ruigrok, S. Romeijn, S. Uleman, C. Oomens, G. Kersten, W. Jiskoot, J. Bouwstra, Diphtheria toxoid and N-trimethyl chitosan layer-by-layer coated pH-sensitive microneedles induce potent immune responses upon dermal vaccination in mice, J Control Release, 262 (2017) 28-36.
23. Z. Ding, E. Van Riet, S. Romeijn, G.F. Kersten, W. Jiskoot, J.A. Bouwstra, Immune modulation by adjuvants combined with diphtheria toxoid administered topically in BALB/c mice after microneedle array pretreatment, Pharm Res, 26 (2009) 1635-1643.
24. P. Johansen, T. Storni, L. Rettig, Z. Qiu, A. Der-Sarkissian, K.A. Smith, V. Manolova, K.S. Lang, G. Senti, B. Mullhaupt, T. Gerlach, R.F. Speck, A. Bot, T.M. Kundig, Antigen kinetics determines immune reactivity, Proc Natl Acad Sci U S A, 105 (2008) 5189-5194.
25. A.C.I. Depelsenaire, S.C. Meliga, C.L. McNeilly, F.E. Pearson, J.W. Coffey, O.L. Haigh, C.J. Flaim, I.H. Frazer, M.A.F. Kendall, Colocalization of cell death with antigen deposition in skin enhances vaccine immunogenicity, J Invest Dermatol, 134 (2014) 2361-2370.
26. S.C. Meliga, C. Flaim, M. Veidt, M.A.F. Kend, The Mechanical Stress Caused by Micro-Projection Arrays Penetrating the Skin for Vaccine Delivery, Australian Journal of Multi-Disciplinary Engineering, 10 (2013).
27. K. Matsuo, Y. Yokota, Y. Zhai, Y.S. Quan, F. Kamiyama, Y. Mukai, N. Okada, S. Nakagawa, A low-invasive and effective transcutaneous immunization system using a novel dissolving microneedle array for soluble and particulate antigens (vol 161, pg 10, 2012), J Control Release, 184 (2014) 9-9.
28. C. Termeer, F. Benedix, J. Sleeman, C. Fieber, U. Voith, T. Ahrens, K. Miyake, M. Freudenberg, C. Galanos, J.C. Simon, Oligosaccharides of Hyaluronan activate dendritic cells via toll-like receptor 4, J Exp Med, 195 (2002) 99-111.
29. C.C. Termeer, J. Hennies, U. Voith, T. Ahrens, J.M. Weiss, P. Prehm, J.C. Simon, Oligosaccharides of hyaluronan are potent activators of dendritic cells, J Immunol, 165 (2000) 1863-1870.
30. M. Leone, S. Romeijn, B. Slutter, C. O'Mahony, G. Kersten, J.A. Bouwstra, Hyaluronan molecular weight: Effects on dissolution time of dissolving microneedles in the skin and on immunogenicity of antigen, Eur J Pharm Sci, 146 (2020) 105269.
31. E.J. Oh, K. Park, K.S. Kim, J. Kim, J.A. Yang, J.H. Kong, M.Y. Lee, A.S. Hoffman, S.K. Hahn, Target specific and long-acting delivery of protein, peptide, and nucleotide therapeutics using hyaluronic acid derivatives, J Control Release, 141 (2010) 2-12.
32. D. Gatto, S.W. Martin, J. Bessa, E. Pellicioli, P. Saudan, H.J. Hinton, M.F. Bachmann, Regulation of memory antibody levels: the role of persisting antigen versus plasma cell life span, J Immunol, 178 (2007) 67-76.
33. G. Crepeaux, H. Eidi, M.O. David, E. Tzavara, B. Giros, C. Exley, P.A. Curmi, C.A. Shaw, R.K. Gherardi, J. Cadusseau, Highly delayed systemic translocation of aluminum-based adjuvant in CD1 mice following intramuscular injections, J Inorg Biochem, 152 (2015) 199-205.
34. R.K. Gupta, Aluminum compounds as vaccine adjuvants, Adv Drug Deliver Rev, 32 (1998) 155-172.
35. M. Vogelbruch, B. Nuss, M. Korner, A. Kapp, P. Kiehl, W. Bohm, Aluminium-induced granulomas after inaccurate intradermal hyposensitization injections of aluminium-adsorbed depot preparations, Allergy, 55 (2000) 883-887.
36. M.L. Mbow, E. De Gregorio, N.M. Valiante, R. Rappuoli, New adjuvants for human vaccines, Curr Opin Immunol, 22 (2010) 411-416.
37. J.C. Joyce, H.E. Sella, H. Jost, M.J. Mistilis, E.S. Esser, P. Pradhan, R. Toy, M.L. Collins, P.A. Rota, K. Roy, I. Skountzou, R.W. Compans, M.S. Oberste, W.C. Weldon, J.J. Norman, M.R. Prausnitz, Extended delivery of vaccines to the skin improves immune responses, J Control Release, 304 (2019) 135-145.
38. V. Bachy, C. Hervouet, P.D. Becker, L. Chorro, L.M. Carlin, S. Herath, T. Papagatsias, J.B.

Barbaroux, S.J. Oh, A. Benlahrech, T. Athanasopoulos, G. Dickson, S. Patterson, S.Y. Kwon, F. Geissmann, L.S. Klavinskis, Langerin negative dendritic cells promote potent CD8+ T-cell priming by skin delivery of live adenovirus vaccine microneedle arrays, Proc Natl Acad Sci U S A, 110 (2013) 3041-3046.

39. C. Edens, M.L. Collins, J.L. Goodson, P.A. Rota, M.R. Prausnitz, A microneedle patch containing measles vaccine is immunogenic in non-human primates, Vaccine, 33 (2015) 4712-4718.
40. A. Pattani, P.F. McKay, R.F. Donnelly, M.J. Garland, K. Migalska, C.M. Cassidy, R. Malcolm, R.J. Shattock, R.M. Curran, Microneedle Mediated Intradermal Delivery of Adjuvanted Recombinant HIV-1 CN54gp140 Effectively Primes Mucosal Boost Inoculations, Aids Res Hum Retrov, 27 (2011) A69-A69.
41. Z. Zhu, X. Ye, Z. Ku, Q. Liu, C. Shen, H. Luo, H. Luan, C. Zhang, S. Tian, C. Lim, Z. Huang, H. Wang, Transcutaneous immunization via rapidly dissolvable microneedles protects against hand-foot-and-mouth disease caused by enterovirus 71, J Control Release, 243 (2016) 291-302.
42. P.A. Buining, A.P. Philipse, H.N.W. Lekkerkerker, Phase-Behavior of Aqueous Dispersions of Colloidal Boehmite Rods, Langmuir, 10 (1994) 2106-2114.
43. A.A. Verhoeff, R.P. Brand, H.N.W. Lekkerkerker, Tuning the birefringence of the nematic phase in suspensions of colloidal gibbsite platelets, Mol Phys, 109 (2011) 1363-1371.

SUPPLEMENTARY MATERIAL

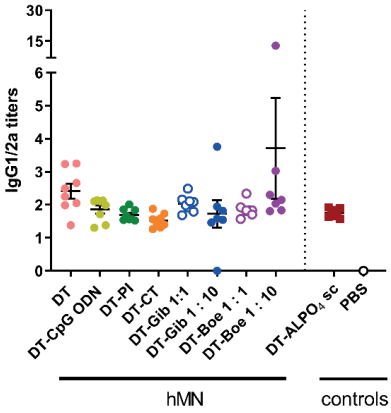

Figure S1. DT-specific IgG1 and IgG2a ratio titers on day 63. Bars represent mean ± SEM, n = 8. No significant difference among the groups was found ($p > 0.05$). hMN, hollow microneedle; DT, diphtheria toxoid; PI, poly(I:C); CT, cholera toxin; Gib, gibbsite; Boe, boehmite; $AlPO_4$, aluminum phosphate.

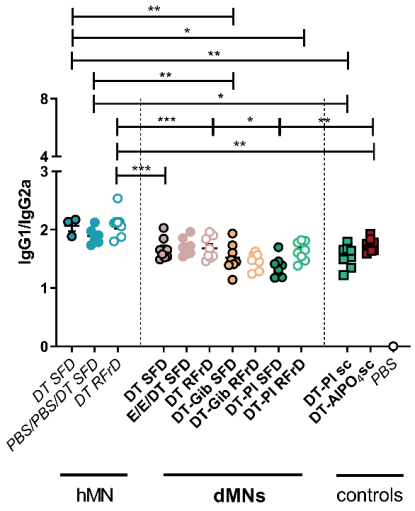

Figure S2. DT-specific IgG1 and IgG2a ratio titers measured in BALB/c mice on day 63. Bars represent mean ± SEM, n = 8. *$p < 0.05$, **$p < 0.01$, ***$p < 0.001$. SFD, single-full dose; RFrD, repeated-fractional dose; dMNs, dissolving microneedles; hMN, hollow microneedle; DT, diphtheria toxoid; PI, poly(I:C); Gib, gibbsite; E, empty dMNs; $AlPO_4$, aluminum phosphate.